[8]Horton, H. P., "Computation of Compressible Laminar Boundary Layers on Swept, Tapered Wings," Queen Mary and Westfield College, Univ. of London, Faculty of Engineering Paper EP-1101, London, June 1995.

[9]Gear, C. W., "The Automatic Integration of Stiff Ordinary Differential Equations," *Information Processing, 68*, edited by A. J. H. Morel, North-Holland, Amsterdam, 1969, pp. 187–193.

Numerical Study of Alternate Forms of Dynamic-Stall-Vortex Suppression

M. C. Towne* and T. A. Buter†
U.S. Air Force Institute of Technology, Wright–Patterson Air Force Base, Ohio 45433

Nomenclature

C_l, C_d, C_m = lift, drag, and moment coefficients
C_μ = blowing coefficient, $\dot{m}_j V_j / q_\infty c$
c = chord
M = Mach number
$\dot{m}_j$ = mass flow rate of jet, $\rho_j s V_j \sin\phi$
q_∞ = dynamic pressure, $\frac{1}{2}\rho_\infty U_\infty^2$
Re_c = chord Reynolds number, $U_\infty c/\nu_\infty$
s = slot width
t^+ = nondimensional time, tU_∞/c
U_∞ = freestream velocity
V_j = velocity of jet
x, y = coordinates of moving reference frame attached to airfoil
α = angle of attack
α_b = onset angle of attack (blowing or suction)
ν = dynamic viscosity
ξ, η = transformed coordinates
ρ = density
ϕ = jet blowing angle, 10 deg
Ω^+ = nondimensional pitch rate, $\omega c/U_\infty$

Introduction

ATTEMPTS have been made by numerous researchers to harness the large aerodynamic forces temporarily generated on a streamlined body rapidly pitched beyond its steady stall angle of attack. Dynamically pitched airfoils exhibit maximum lift coefficients two or three times the static maximum lift.[1] Uncontrolled, the ensuing unsteady motion results in dynamic stall. The dynamic stall phenomenon arises in several applications: wind turbine blades, helicopter rotor blades, jet engine compressor blades, and rapidly pitched airfoils. The current study compares and contrasts two approaches to dynamic stall suppression: 1) suction and 2) nearly tangential blowing, applied in the vicinity of the leading edge of a NACA 0015 airfoil.

Dynamic stall suppression via leading-edge suction and leading-edge tangential blowing focuses on the removal of low momentum fluid that accumulates along the airfoil upper surface as it is pitched upward. Specifically, as the airfoil is pitched up, the adverse pressure gradient along the upper surface promotes the forward propagation of reverse-flowing fluid into the leading-edge region. The thickening of this low momentum fluid region near the leading edge ultimately forces an upward displacement and "kinking" of the feeding shear layer. The kinking of this shear layer marks the initial formation of the dynamic stall vortex. Suction experiments by Karim and Acharya[2] demonstrated that the key to dynamic-stall-vortex-formation suppression is to remove fluid from underneath the leading-edge-originating shear layer at the same rate as the reverse-flowing-fluid-pooling accumulation rate. Results by Towne[3] verify their findings numerically and demonstrate that tangential blowing applied upstream and/or in this pooling region is also effective in eliminating the low momentum region, and hence, in delaying dynamic stall vortex (DSV) formation.

The flow regime of interest is one of low speed and low Reynolds number. A compressible Navier–Stokes code developed by Visbal to numerically investigate dynamic stall[4,5] is used. The nominal flow and pitch-rate conditions are $M_\infty = 0.2$, $Re_c = 2.4 \times 10^4$, and $\Omega_0^+ = 0.2$.

Numerical Methodology

The strong conservation law form of the two-dimensional compressible Navier–Stokes equations are cast in an inertial frame of reference using a general time-dependent coordinate transformation to account for the motion of the body. Closure of the system is provided by the perfect-gas law, Sutherland's viscosity formula, and the assumption of a constant Prandtl number.

Freestream conditions are imposed at the inflow boundary. At the surface, no-slip adiabatic conditions are used. At the outflow far-field boundary, velocity and density are extrapolated and pressure is set to the freestream pressure. For the current simulation, an O-grid structure is employed. This necessitated the specification of periodic boundary conditions at the O-grid cut by overlapping five grid points in the ξ direction. To simulate the nearly tangential jet the velocity at the slot location was specified with a given magnitude and orientation. The pressure boundary condition was not modified at the slot. The flowfield for time-periodic flow at zero angle of attack is used as the initial condition.

To avoid the expense of regridding at every time level, a grid that is fixed relative to the airfoil was used. An extensive grid study was conducted on mesh sizes ranging from 203 to 505 points in the ξ direction (circumferential) and 101 to 301 points in the η direction.[3] Each grid was applied to a physical domain that extends nominally 30 chord lengths away from the airfoil. The current results were obtained on a 361×201 grid that had minimum ξ and η spacings of 0.000082 and $0.00005c$, respectively. No fewer than 21 grid points were used to define the slot aperture. The governing equations were numerically solved using the alternating direction implicit approximate-factorization algorithm of Beam and Warming.[6] Fourth-order explicit and second-order implicit spectral damping was used to damp high-frequency numerical oscillations and enhance stability behavior.

Results and Discussion

In a previous numerical study by Towne,[3] nearly tangential blowing was applied at a series of locations along the airfoil upper surface to assess the effect of slot position on DSV suppression. Based upon this work and the suction experiment of Karim and Acharya,[2] the comparison between suction and blowing was conducted for a single slot position of width $0.00717c$ at $x/c = 0.05$. The selection of this position assured that the slot was located upstream of the point at which the DSV was seen to form in the natural (no-control) case. Previous work by Towne and Buter[7] showed that blowing applied aft of the natural DSV vortex formation point, while useful for retarding the forward propagation of reverse flow from the trailing edge, did not suppress the formation of the dynamic stall vortex.

Received April 12, 1995; revision received May 16, 1995; accepted for publication May 16, 1995.

*Assistant Professor. Member AIAA.
†Assistant Professor. Senior Member AIAA.

Previous work[2,4] has shown that suction effectiveness is tied to the removal of low momentum fluid that pools along the upper surface as the airfoil is pitched upward. Thus, its effectiveness is dependent upon the mass flow rate at which this fluid is removed. In contrast, blowing suppresses dynamic stall vortex formation by adding momentum to the fluid near the surface; in effect adding momentum to the feeding shear layer. Thus, its effectiveness is clearly tied to variations in C_μ. Therefore, for a fixed jet velocity, blowing through smaller slot widths is more effective, to the limit of choked slot flow. The dependence of suction and blowing on different problem parameters complicates the comparative process. In the current study, no attempt was made to optimize slot width for blowing.

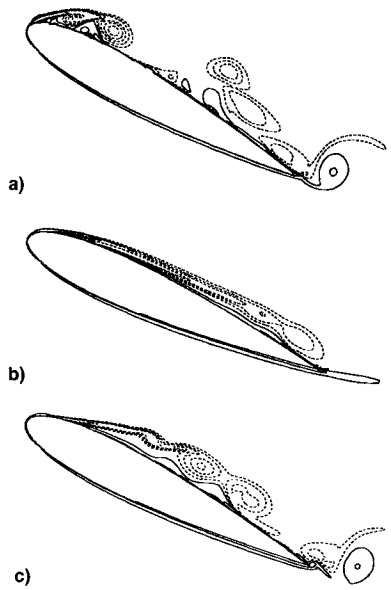

Fig. 1 Isovorticity contours for natural case, tangential-blowing control, and suction control at 0.05c slot; α = 27 deg, $\dot{m}$ = 0.0051 $\rho_\infty U_\infty c$ for blowing and suction: a) natural, b) v_j = 4.14U_∞, and c) v_s = 0.72U_∞.

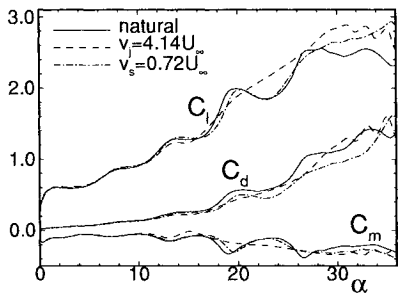

Fig. 2 C_l, C_d, and C_m (about X = 0.25c) comparisons for natural case, tangential-blowing control, and suction control at 0.05c slot; $\dot{m}$ = 0.0051$\rho_\infty U_\infty c$ for blowing and suction.

Results for $\dot{m}$ = 0.0051$\rho_\infty U_\infty c$ corresponding to a suction velocity of 0.72U_∞ and a blowing velocity of 4.14U_∞ (C_μ = 0.246; blowing was applied at a 10-deg angle relative to the surface) are presented in Fig. 1. For the test conditions considered, without control a DSV begins to form at α = 21 deg. Both techniques effectively suppress the formation of the dynamic stall vortex, though for this geometry and $\dot{m}$, suction delays DSV formation by an additional 2 deg. Examination of the vorticity field along the upper surface indicates that blowing strengthens the shear layer, thereby delaying a amalgamation into distinct vortical structures downstream of the leading edge. Suction, while acting to promote attached flow along the leading edge, is less effective in sustaining a coherent shear layer along the upper surface. The consequence of this is clearly illustrated in the aerodynamic coefficient information presented in Fig. 2. The formation and shedding of shear-layer vortices along the airfoil upper surface in both the natural and suction cases manifests itself as an oscillation in pitching moment (computed about the quarter-chord); this effect is greatly reduced when blowing is applied. Note that the high momentum fluid added by blowing increases both the lift and drag coefficient.

The angle of attack at which control was initiated was also investigated. Researchers[2,8] have shown that the successful suppression of DSV formation via suction or nearly tangential blowing can be achieved even when control is not initiated at the beginning of the pitch-up cycle. The effect of suction and blowing initiation angle is presented in Fig. 3 at α = 27 deg (roughly 6 deg after the DSV forms in the uncontrolled case). For the conditions investigated, the structure of the shear layer at this angle of attack is virtually unaltered by a variation of α_b, provided blowing is initiated prior to the natural DSV onset angle. This angle is telegraphed by the appearance of a flattening in the upper surface pressure distribution at the location where the DSV subsequently forms.[8]

While delays in suction implementation are likewise effective in suppressing DSV formation, changes in α_b manifest themselves in the form of structural variations in the shear layer aft of the midchord. This underscores the causal difference between suction and blowing. As previously noted, blowing increases the strength of the shear layer by adding high momentum fluid, whereas suction acts to stabilize the shear layer by delaying its outward displacement and kinking, rather than actually increasing its strength. Thus, the suction-altered shear layer is more susceptible to breakdown than the stronger shear layer created by blowing. Again note that once a DSV is formed, suction and blowing as implemented are ineffective, at least in so far as DSV formation/suppression is concerned.

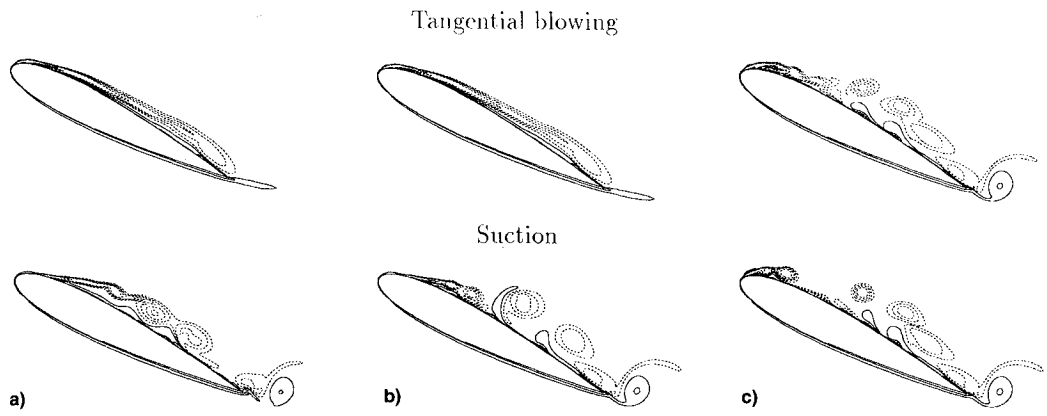

Fig. 3 Effect of a variation in α_b (α = 27 deg); $\dot{m}$ = 0.0051$\rho_\infty U_\infty c$, for slot at 0.05c. α = a) 0, b) 20, and c) 22 deg.

Acknowledgment

The authors would like to thank Miguel Visbal for a number of helpful suggestions.

References

[1]Jumper, E., Schreck, S., and Dimmich, R., "Lift-Curve Characteristic for an Airfoil Pitching at Constant Rate," *Journal of Aircraft*, Vol. 24, No. 10, 1987, pp. 680–687.

[2]Karim, M., and Acharya, M., "Control of the Dynamic-Stall Vortex over a Pitching Airfoil by Leading-Edge Suction," AIAA Paper 93-3267, July 1993.

[3]Towne, M., "Numerical Simulation of Dynamic Stall Suppression by Tangential Blowing," PhD. Dissertation, U.S. Air Force Inst. of Technology, Wright–Patterson AFB, OH, 1994.

[4]Visbal, M., "On the Formation and Control of the Dynamic Stall Vortex on a Pitching Airfoil," AIAA Paper 91-0006, Jan. 1991.

Visbal, M., "Dynamic Stall of a Constant-Rate Pitching Airfoil," *Journal of Aircraft*, Vol. 27, No. 5, 1990, pp. 400–407.

[6]Beam, R., and Warming, R., "An Implicit Factored Scheme for the Compressible Navier-Stokes Equations," *AIAA Journal*, Vol. 16, No. 4, 1978, pp. 393–402.

[7]Towne, M., and Buter, T., "Numerical Simulation of Dynamic-Stall Suppression by Tangential Blowing," AIAA Paper 94-0184, Jan. 1994.

[8]Towne, M., and Buter, T., "Dynamic Stall Suppression by Nearly Tangential Blowing: Navier-Stokes Computations," *AIAA Journal* (submitted for publication).

Estimation of the Moment Coefficients for Dynamically Scaled, Free-Spinning Wind-Tunnel Models

C. M. Fremaux*
Lockheed Engineering and Sciences Company, Inc., Hampton, Virginia 23666

Nomenclature

b	=	wingspan, ft
$\bar{c}$	=	mean aerodynamic chord, ft
I_x, I_y, I_z	=	model moments of inertia about the X-, Y-, or Z-body axis, respectively, slug-ft^2
I_{xz}, I_{yx}, I_{yz}	=	model products of inertia, slug-ft^2
l	=	total aerodynamic rolling moment about c.g., coefficient $C_l = l/\hat{q}Sb$
m	=	total aerodynamic pitching moment about c.g., coefficient $C_m = m/\hat{q}S\bar{c}$
n	=	total aerodynamic yawing moment about c.g., coefficient $C_n = n/\hat{q}Sb$
p	=	angular rate about X-body axis, rad/s
q	=	angular rate about Y-body axis, rad/s
$\hat{q}$	=	freestream dynamic pressure, $\frac{1}{2}\rho V^2$, lb/ft^2
R	=	spin radius: distance from model c.g. to spin axis, ft
r	=	angular rate about Z-body axis, rad/s
S	=	wing area, ft^2
V	=	vertical wind-tunnel freestream velocity, ft/s
α'	=	angle between X-body axis and vertical in vertical wind tunnel, deg or rad
ρ	=	air density, slugs/ft^3
ψ, θ, ϕ	=	Euler angles: azimuth, pitch, and roll angles, respectively, deg or rad
Ω	=	spin rate, i.e., angular velocity about vertical axis, deg/s or rad/s

Received April 20, 1995; revision received May 19, 1995; accepted for publication May 30, 1995.

*Engineer, Advanced Aircraft and Flight Dynamics Section, 144 Research Drive. Senior Member AIAA.

Introduction

AERODYNAMIC forces and moments on a model undergoing steady rotation at a constant attitude can currently be measured using the rotary balance technique.[1,2] These data are used to predict potential steady spin modes and for building up data bases for the spin portion of flight simulations. However, rotary balance data alone cannot be used to predict oscillatory spins since the measured forces and moments are constant for a given set of conditions. In contrast, dynamically scaled free-spinning models can predict the oscillatory nature of an airplane's spin.[1]

Free-spin tests of dynamically (Froude) scaled models have been performed in the NASA Langley 20-ft Vertical Spin Tunnel since 1941.[1] In all of these tests, model attitude and angular rate data were obtained from high-speed motion picture film or video tape records, read frame-by-frame, to quantify spin modes. Historically, this method has been used successfully to predict full-scale results. However, 6-degree-of-freedom time histories of model motions have recently become available via a computerized, optically-based data acquisition system known as the Spin Tunnel Model Space Positioning System (MSPS).[3] Using the equations of motion coupled with these time histories, a simple procedure for estimating the moment coefficients about all three body axes during a spin that may or may not be oscillatory is developed. The method used in this Note is similar to that proposed by Neihouse et al.[1] for determining the moments of a spinning airplane from flight-test data.

Estimation of Moment Coefficients

For a true equilibrium spin mode to exist (i.e., a "steady" spin in which the angular accelerations are equal to zero), the external (aerodynamic) moments and inertial moments about all three axes must balance simultaneously. In many cases, assuming that a spin is steady is reasonable since the angular accelerations are small and can be ignored. In reality, however, no spin is perfectly steady and, in fact, some may be quite oscillatory. Free-spin tests with dynamically scaled models provide a unique opportunity to determine the moments produced during an oscillatory spin.

In terms of the equations of motion for a rigid body (assuming a body axis system is used in which $I_{yx} = I_{yz} = 0$), the moment balance, including angular accelerations, can be written as

$$l = I_x\dot{p} - I_{xz}\dot{r} + (I_z - I_y)rq - I_{xz}pq \tag{1}$$

$$m = I_y\dot{q} - (I_z - I_x)pr + I_{xz}(p^2 - r^2) \tag{2}$$

$$n = I_z\dot{r} - I_{xz}\dot{p} + (I_y - I_x)pq + I_{xz}rq \tag{3}$$

where a superscript dot over a variable represents differentiation with respect to time. Assuming with $\psi = R = 0$ and rewriting the body-axis angular rates in terms of the Euler angles and the spin rate yields

$$p = -\Omega \sin\theta \tag{4}$$

$$q = \Omega \cos\theta \sin\phi \tag{5}$$

$$r = \Omega \cos\theta \cos\phi \tag{6}$$

Differentiating Eqs. (4–6) with respect to time, substituting